Carbohydrate Polymers 338 (2024) 122172

Contents lists available at ScienceDirect

Carbohydrate Polymers

journal homepage: www.elsevier.com/locate/carbpol

Synthesis and real-time characterization of self-healing, injectable, fast-gelling hydrogels based on alginate multi-reducing end polysaccharides (MREPs)

Zhenghao Zhai [a], Yang Zhou [b], Ishani Sarkar [e], Yang Liu [a], Yimin Yao [a,c], Junru Zhang [d], Michael J. Bortner [a,c], John B. Matson [a,e], Blake N. Johnson [a,c,d], Kevin J. Edgar [a,b,*]

[a] Macromolecules Innovation Institute, Virginia Tech, Blacksburg, VA 24061, United States
[b] Department of Sustainable Biomaterials, Virginia Tech, Blacksburg, VA 24061, United States
[c] Department of Chemical Engineering, Virginia Tech, Blacksburg, VA 24061, United States
[d] Department of Industrial & Systems Engineering, Virginia Tech, Blacksburg, VA 24061, United States
[e] Department of Chemistry, Virginia Tech, Blacksburg, VA 24061, United States

ARTICLE INFO

Keywords:
Polysaccharides
Multi-reducing end polysaccharides (MREPs)
Hydrogels
Self-healing
Cantilever sensor
Alginate
Polyethyleneimine

ABSTRACT

Polysaccharide-based hydrogels are promising for many biomedical applications including drug delivery, wound healing, and tissue engineering. We illustrate herein self-healing, injectable, fast-gelling hydrogels prepared from multi-reducing end polysaccharides, recently introduced by the Edgar group. Simple condensation of reducing ends from multi-reducing end alginate (M-Alg) with amines from polyethylene imine (PEI) in water affords a dynamic, hydrophilic polysaccharide network. Trace amounts of acetic acid can accelerate the gelation time from hours to seconds. The fast-gelation behavior is driven by rapid Schiff base formation and strong ionic interactions induced by acetic acid. A cantilever rheometer enables real-time monitoring of changes in viscoelastic properties during hydrogel formation. The reversible nature of these crosslinks (imine bonds, ionic interactions) provides a hydrogel with low toxicity in cell studies as well as self-healing and injectable properties. Therefore, the self-healing, injectable, and fast-gelling M-Alg/PEI hydrogel holds substantial promise for biomedical, agricultural, controlled release, and other applications.

1. Introduction

Hydrogels are three-dimensional networks crosslinked by hydrophilic polymers, which can hold large amounts of water. Because of structural similarities, hydrogels have properties akin to those of many soft tissues (Patenaude et al., 2014) and are widely used in biomedical applications such as in drug delivery systems (Hoare & Kohane, 2008; Li & Mooney, 2016; Zhou et al., 2023), wound dressings (Pan et al., 2021; Tavakoli & Klar, 2020) or scaffolds for tissue engineering (Drury & Mooney, 2003; Lee & Mooney, 2001). Hydrogels historically were preformed in vitro and then delivered to target sites using invasive surgical procedures (Dimatteo et al., 2018). In recent decades, injectable hydrogels have been prepared, fueling significant recent research efforts (Sun et al., 2020). Injectability makes it possible for medical personnel to introduce hydrogels to target sites in the body by minimally invasive procedures. Besides the requirements that they do not cause harm to surrounding tissues, do not elicit immune responses, and biodegrade in an appropriate time frame, injectable medical hydrogels should undergo rapid sol–gel transition after injection to achieve and maintain sufficient strength and integrity, for a duration suitable for the particular application at the target site in vivo (Guvendiren et al., 2012).

Physically crosslinked injectable hydrogels have been developed for controlled release and tissue engineering, but undesirably rapid erosion in aqueous environments limited their application (Shen et al., 2006). Chemically crosslinked hydrogels relying on covalent bonds are more stable. Covalently crosslinked hydrogels have been formed by methods including Diels–Alder reactions, Schiff base formation, thiol/disulfide redox reactions, and click chemistry (Alonso et al., 2021; Chen et al., 2022). Schiff-base hydrogels have shown great promise because they are typically self-healing due to their dynamic imine bonds (Chen et al., 2020; Zhou et al., 2023) formed by condensation of aldehydes or ketones with amines, forming water as sole by-product (hence reversible in

* Corresponding author at: Macromolecules Innovation Institute, Virginia Tech, Blacksburg, VA 24061, United States.
E-mail address: kjedgar@vt.edu (K.J. Edgar).

https://doi.org/10.1016/j.carbpol.2024.122172
Received 1 September 2023; Received in revised form 13 April 2024; Accepted 15 April 2024
Available online 19 April 2024
0144-8617/© 2024 Elsevier Ltd. All rights reserved.

the presence of the vast excess of water present in a hydrogel). Due to their ability to self-repair, dynamic properties of Schiff-base linked hydrogels can partly compensate for hydrogel mechanical properties that may be insufficient for some biomedical applications (Gyarmati et al., 2017). Polysaccharides are abundant, sustainable, diverse, and typically benign. In general, they do not elicit strong immune responses. For these reasons among others, they are highly attractive substrates for hydrogel synthesis. However, preparation of polysaccharide-based injectable Schiff-base hydrogels typically begins with periodate oxidation of the polysaccharide chain, whereby vicinal diols are cleaved to dialdehydes, thus opening monosaccharide rings (Hozumi et al., 2018; Malik et al., 2022; Yang et al., 2019). While providing ample aldehyde functionality for crosslinking, this method reduces polysaccharide rigidity, leading also to lower degree of polymerization (DP), greater chemical instability, and degraded mechanical properties (Kristiansen et al., 2010). What's more, the gelation time of Schiff-base hydrogels is usually from minutes to hours due to the nature of the reversible dynamic bonds (Chen et al., 2022; Mo et al., 2021; Yang et al., 2022). How can these issues be addressed?

Development of multi-reducing end polysaccharides (MREPs) has made it possible to address the drawbacks of the periodate oxidation approach. Recently, we reported a strategy to synthesize MREPs by linking the 2-amino-2-deoxy moieties of glucosamine to polysaccharide chains. The amide-linked glucosamines are in equilibrium between a ring-closed hemiacetal and an open-chain aldehyde form. This method introduces more reducing ends (aldehyde groups) to the polysaccharide chains without damaging the cyclic structures of the monosaccharides. Based on our previous research, Schiff-base hydrogels can be obtained by mixing a multi-reducing end alginate (M-Alg) solution with branched polyethyleneimine (PEI) solution at room temperature. In a control experiment, no hydrogel was formed upon mixing a solution of unmodified alginate with a PEI solution (Zhai et al., 2023). However, gelation of the same concentrations and proportions of alginate MREP with PEI was consistently rather slow, requiring ca. 24 h; this rate is not practical for many medical (or other) uses. To speed up the gelation process, we proposed to make use of the fact that the reducing end of the appended glucosamine is mainly in its glucopyranose ring, hemiacetal form, and that its conversion to the acyclic (aldehyde) form is accelerated in the presence of free hydrogen ions (Qian, 2013). In addition, Schiff-base bond formation is known to be accelerated by weak acids, including acetic acid (Cordes & Jencks, 1962; Santerre et al., 1958). Therefore, we hypothesized that gelation of multi-reducing end alginate (M-Alg) with polyethyleneimine (PEI) could be accelerated to biomedically useful rates by adding trace amounts of acetic acid. We further hypothesized that the fast-gelling M-Alg/PEI hydrogel should also have self-healing and injectable properties. Upon adding the acetic acid, we expect that aldehyde groups will be rapidly generated by ring-opening of the appended glucosamines, priming the MREPs for crosslinking with amine-containing polymers like PEI through accelerated Schiff base chemistry. What's more, the acetic acid will also protonate PEI amine groups, which can associate with M-Alg carboxylates through ionic interactions (Rajabi et al., 2021; Tian et al., 2020). Acetic acid would thereby act as a multifunctional catalyst to achieve combined physically and chemically crosslinked, polysaccharide-based hydrogels with self-healing, injectable, and fast gelation properties. Herein we report the results of testing these hypotheses.

2. Experimental

2.1. Materials

Alginic acid sodium salt (M/G ratio 1.9, $M_n = 1.09 \times 10^5$ g/mol (Zhai et al., 2023)) was from Alfa Aesar. Polyethyleneimine (PEI, branched, $M_n \sim 10{,}000$ reported by the manufacturer), (4-(4,6-dimethoxy-1,3,5-triazin-2-yl)-4-methylmorpholinium chloride (DMTMM) ($\geq$ 96 %) and D-(+)-glucosamine hydrochloride (GlcN:HCl) were from Sigma-Aldrich. DI water (~18.2 MΩ·cm) was produced by a Synergy instrument from Millipore company. All reagents were used without further purification. Regenerated cellulose dialysis tubing (molecular weight cutoff (MWCO) 3.5 kDa) was from Fischer Scientific.

2.2. NMR measurements

^{1}H and ^{13}C NMR spectra were obtained on either Bruker Avance 500 or 600 MHz spectrometers, using 128 scans for ^{1}H NMR and 10,000 scans for ^{13}C NMR. Samples were analyzed in D_2O using standard 5 mm o.d. tubes. ^{1}H NMR spectra of alginate-based polymers were referenced to D_2O (4.79 ppm).

2.3. Determination of the degree of substitution of glucosamine (DS (GlcN)) of M-Alg

DS (GlcN) was determined based on our previously published method (Zhai et al., 2023), calculated by peak integration ratios (^{1}H NMR spectroscopy, Fig. S1).

$$\frac{2 \times \mathrm{DS(GlcN)}}{1} = \frac{\mathrm{I}(a\alpha) + \mathrm{I}(d\alpha + d\beta + e\beta)}{\mathrm{I(G1)} \times (1 + \mathrm{M/G\ ratio})} \quad (2)$$

Letters correspond to those in Fig. S1.

2.4. Synthesis of multi-reducing end alginate (M-Alg)

The synthesis procedure was modified from our previously published method (Zhai et al., 2023). Alginic acid sodium salt (1.5 g, 6.3 mmol –COONa) was first dissolved in DI water (250 mL) in a 500 mL round bottom flask at room temperature under magnetic stirring overnight. After complete dissolution, the temperature was raised to 37 °C and DMTMM (1.72 g, 6.2 mmol, 1 equiv. per –COONa) was added to the solution. After 3 h stirring at 37 °C, D-(+)-glucosamine hydrochloride (4 g, 18.6 mmol, 3 equiv. per –COONa) was added and the pH was adjusted to 8 using dilute aq. NaOH. The solution was stirred at 37 °C for 24 h. The reaction mixture then was transferred to a dialysis tube (cutoff 3.5 kDa) and dialyzed against 0.1 M NaCl for 2 d, then against DI water for 3 d. Products were obtained by freeze drying to afford a white fibrous material (0.96 g, yield: 60 %).

2.5. General procedure for fabrication of M-Alg/PEI hydrogel

M-Alg (0.05 g) and PEI (1.00 g) were dissolved in separate 1 mL portions of DI-water overnight to afford 5 % w/v M-alg and 50 % w/w PEI solutions. Then the two solutions were combined and 5 μL acetic acid was added. The solutions were vortexed for 10 s, with gelation occurring within seconds. Gelation was defined as lack of flow. Hydrogels were light orange in color.

2.6. Real-time rheological analysis of M-Alg/PEI hydrogel using a cantilever rheometer

The rheological properties of synthesized hydrogels were characterized using dynamic-mode piezoelectric milli-cantilever (PEMC) sensor, given the ability of such sensors to characterize hydrogel rheological properties in low-volume, continuous monitoring applications. PEMC sensors were fabricated as previously reported (Cesewski et al., 2020; Haring et al., 2020; Liu et al., 2022; Sharma et al., 2011; Singh et al., 2021; Zhang et al., 2023). Continuous monitoring of the cantilever resonant frequency and phase angle was performed using an impedance analyzer (e5061b; Keysight) and custom Matlab program for data acquisition. Each sample was tested at least three times. Five cantilevers with similar spectral features (e.g., resonant frequency) were used in the study.

Precursor solutions for sensor tests were prepared by combining M-Alginate (5 % w/v) and PEI stock solutions (50 % w/w) to get a specific

ratio between polymers. The precursor solutions (including AcOH if it was contained in the formulation) were thoroughly mixed by vortex followed by centrifuging at 3000 rpm for 3 min to eliminate bubbles before tests. For real-time monitoring experiments, the mass ratio of M-Alginate:PEI = 1:1. A sensor tip was first immersed in the sol solution (0.8 mL) to obtain a steady baseline, and then 5 μL of AcOH was added near the sensor tip to trigger the gelation process. Monitoring was continued until a steady plateau was reached with regard to phase angle. The effect of mass ratio on viscoelastic properties of hydrogels was studied by preparing precursor solutions having different mass ratios of M-alginate and PEI (1:1, 1:3, 1:5, 1:7, 1:9). The amount of added acetic acid was also varied (0, 5, 10, 15 μL) to study its effect on hydrogel properties at a mass ratio of M-Alginate to PEI (1:10). In these two cases, the precursor solutions were sealed and stored at room temperature for 18 h to form hydrogels. The obtained hydrogels were analyzed by immersing a sensor into the hydrogels to perform spectrum sweeps at least five times. Sensor test results were further analyzed by converting the PEMC sensor data to mechanical property information (i.e., G′) by using a fluid-structure interaction model (Cesewski et al., 2020; Liu et al., 2022; Mather et al., 2012).

2.7. Analysis of M-Alg/PEI hydrogel self-healing properties using parallel plate rheometer

Rheological experiments were performed on a TA Instruments AR-G2 rheometer with 25 mm parallel plate geometry and temperature-controlled Peltier plate (25 °C). In frequency sweep experiments, strain was set at 1 %. In strain sweep experiments, frequency was set at 0.1 Hz. In alternating step-strain sweep experiments, frequency was set at 0.1 Hz. Strain was set as 1 % and 100 %. Hydrogels were subjected to 1 % strain for 5 min, then strain was increased to 100 % and kept at that level for 5 min, then strain was restored to 1 %. These cycles of two alternating steps were repeated five times. Hydrogels for rheological experiments were prepared from aqueous solutions of 5 % w/v M-Alg and 50 % w/w PEI with 5 μL acetic acid.

2.8. Cytotoxicity

Cell studies were conducted using L929 cells (adherent mouse fibroblast cells; ATCC catalog number CCL-1) at passages 14–18. Cultures were grown in Dulbecco's modified eagle medium (DMEM) supplemented with 10 % fetal bovine serum (FBS), 50 IU/mL penicillin, and 50 μg/mL streptomycin (MP Biomedicals). Cells were cultured at 37 °C in 5 % CO_2 air. Medium was changed every other day. After 80–90 % confluence was achieved, the cells were passaged. Cells were washed with 1× PBS three times, and then released with 0.05 % trypsin-EDTA solution (VWR, Radnor, PA). The suspension of released cells was centrifuged at 200 ×*g* (1000 rpm) for 5 min before counting and plating for experiments.

For the cytotoxicity of M-Alg and PEI, L929 cells were seeded in a 96-well plate at a density of 5000 cells per well in 200 μL serum-containing DMEM (with phenol red) per well. The cells were cultured for 24 h after which the media was discarded, and the cells were washed three times with 1× PBS. Stock solutions of PEI (1 mg/mL) and M-Alg (20 mg/mL) were prepared by dissolving the desired amounts of PEI and M-Alg in DMEM. Next, varying concentrations of PEI (5 μg/mL to 80 μg/mL) and M-Alg (0.1 mg/mL to 10 mg/mL) were prepared from each stock solution. 200 μL of each solution was added to the seeded cells, and the cells were incubated for 24 h. After incubation, the cells were washed with PBS three times and then treated with serum-free DMEM (100 μL). Next, 10 μL of cell counting kit 8 solution (CCK8, Dojindo, Rockville, MD) was added to each well. The CCK8 dye was allowed to develop by incubating for 3 h after which the absorbance was recorded at 450 and 750 nm using a BioTek Synergy Mx plate reader (Biotek, Winooski, VT). Worked-up data (absorbance at 750 nm subtracted from absorbance at 450 nm) were graphed using Microsoft Excel. Mean values are reported together with the standard deviation (SD) representing the combination of 3 independent experimental runs with three replicates per experiment.

For the hydrogel preparation, vials containing 50 mg of lyophilized M-Alg and 200 mg of PEI were sprayed with 70 % ethanol in water and sterilized under UV light inside a biosafety hood for at least 2 h. The M-Alg was dissolved in 1 mL PBS, and the PEI was dissolved in 2 mL PBS inside the biosafety hood. The solutions were left in the biosafety hood overnight to allow the M-Alg to dissolve. Next, 50 μL of the 100 mg/mL PEI solution was added to the entire 50 mg/mL M-Alg solution and mixed well using a vortex. Next, 55 μL of 1 M HCl was added to adjust the pH to ~7.5, and the mixture was vortexed to form the hydrogel. The hydrogel was carefully removed from the vial using a plastic pipette and smeared at the bottom surface of several wells in a 48-well plate such that it coated the entire bottom of the wells. The well plate was sterilized under UV light in the biosafety hood for ca. 45 min.

L929 cells were seeded on top of the hydrogels in the 48-well plate at a density of 10,000 cells per gel with 200 μL of DMEM supplemented with 2 % FBS. Cells were cultured in an incubator for 1 h, 2 h, 5 h and 24 h. The live/dead combined solution (Molecular Probes L3224) was prepared by adding 2 μL of EthD-1 stock solution (component B) to 1 mL PBS. The solution was vortexed, and 1 μL of 4 mM calcein AM stock solution (component A) was added to the solution and vortexed well to prepare a final live/dead staining solution (4 μM calcein AM and 4 μM EthD-1). After the desired incubation times, 40 μL of the live/dead solution was added to each well, and cells were incubated for another 45 min. The gels were then visualized using a bright field and fluorescent microscope (Nikon Eclipse Ti—U) with FITC (for viewing live cells as green spots) and TRITC (for viewing dead cells as red spots) filter set. The magnification was 10×.

3. Results and discussion

3.1. Synthesis and characterization of M-Alg, and hydrogel formation

Synthesis of M-Alg followed our previous paper (Zhai et al., 2023), and the alginate decorated by amide-linked 2-amino-2-deoxyglucose moieties (M-Alg) was characterized by ^{1}H NMR (Fig. S1). Water suppression NMR was conducted to quantify the anomeric α-H resonance of the appended glucosamine (GlcN). This enabled accurate peak integration and further calculation of DS(GlcN) of M-Alg. Based on ^{1}H NMR spectrum integration and Eq. 2, DS(GlcN) of M-Alg was calculated to be 0.4, which is to say that 40 % of the uronic acid monosaccharides of alginate had glucosamine substituents appended via amide linkages to the uronic acid carbonyls, which we predicted would be sufficient for crosslinking with PEI through Schiff base chemistry.

Our previous research confirmed that 5 % w/v M-Alg could form hydrogels with 50 % w/w branched PEI at room temperature after 24 h. To prove that gelation was mainly due to Schiff base crosslinks, we carefully made Alg and M-Alg solutions at the same concentration (5 % w/v). Acetic acid was used to adjust the pH of Alg solution to be the same as that of M-Alg solution (around 6.5). Then 5 % w/v Alg and M-Alg solutions were mixed separately with 50 % w/w branched PEI solution at room temperature. After 24 h, a hydrogel was formed from the M-Alg/PEI mixture while no gelation was observed in the Alg/PEI mixture (Fig. S2). Final pH values of both the M-Alg/PEI and Alg/PEI mixtures were around 8.5. Ionic interactions at this slightly basic pH should be weak since <50 % of the amine groups should be protonated (Kong & Mooney, 2003). The appended glucosamine of M-Alg is in equilibrium between a ring-closed hemiacetal and an open-chain aldehyde form. The abundant amine groups of branched PEI can react with these open-chain aldehydes, thus pushing the hemiacetal-aldehyde equilibrium towards the aldehyde, finally forming a hydrogel. The Schiff base reaction between multi-reducing end alginate and molecules with amine groups was further confirmed by reacting M-Alg with small molecules, by conjugating with the amino acid valine using $NaBH_3CN$ as the reducing agent. Cyanoborohydride reduced the dynamic imines to

saturated, stable amines. After 48 h of reaction and dialysis against water for >7 days, the ^{1}H NMR of the final product revealed a distinguishable peak at around 2 ppm, which was assigned to the methyl peaks from valine (Fig. S3). This evidence strongly supports the contention that M-Alg can react with molecules with amine groups through Schiff base chemistry.

To accelerate the gelation process, a trace amount of acetic acid was used both to catalyze ring-opening of the appended glucosamine and Schiff base formation, and to protonate the amines, thus inducing ionic interactions with alginate carboxylates (Cordes & Jencks, 1962; Kong & Mooney, 2003; Rajabi et al., 2021; Santerre et al., 1958; Tian et al., 2020). The proposed gelation mechanism is displayed in Fig. 1. We observed (Fig. 2) that the M-Alg/PEI solutions could still flow after mixing. But after adding 5 μL acetic acid and vortexing, a hydrogel was formed within <10 s. The weak acid-catalyzed method not only promises to provide fast gelation for polysaccharide-based hydrogels, but also enables thorough mixing of the two polymer components, avoiding any inhomogeneity and/or insufficient crosslinking density of the hydrogel. The FT-IR spectrum of the gel exhibited characteristic peaks from both M-Alg (C—O—C stretching peak at 1030 cm^{-1}) and PEI (C—H stretching peak at 2806 cm^{-1}) (Fig. S7).

3.2. Real-time sensor-based monitoring of M-Alg/PEI gelation

The dynamic gelation process provides a direct, vivid, visual perspective for studying hydrogels (e.g., kinetics of formation). However, conventional characterization methods often face challenges regarding process integration and continuous monitoring of gelation processes in low-volume and high-throughput experimental formats (Liu et al., 2022; Yue et al., 2023; Zhang et al., 2023) (e.g., via rheological property monitoring), which drives the creation of sensor-based methods for material property characterization. Here, we used a sensor-based milli-cantilever rheometer to continuously monitor the gelation process and simultaneously characterize the effect of hydrogel composition on the storage modulus. Schematics of the cantilever sensor design and measurement format are shown in Fig. 3. We first monitored the viscoelastic property response of the M-Alg/PEI hydrogel to acetic acid. Fig. 4a shows the frequency response of the PEMC sensor before and after gelation. The significant decrease in phase angle caused by acetic acid addition is consistent with a gelation process-induced damping effect based on previous studies with alginate hydrogels (Haring et al., 2020; Liu et al., 2022). M-Alg/PEI gelation was next monitored in real-time via continuous tracking of the cantilever Φ. As shown in Fig. 4b, the Φ changed rapidly upon addition of acetic acid and stabilized at a new baseline in <20 min, which is consistent with the visually observable acid-catalyzed gelation process (Fig. 2).

Having established the sensor-based low-volume characterization format for continuous monitoring of M-Alg/PEI rapid hydrogel gelation dynamics, we next examined the effect of mass ratio (M-Alg:PEI) and amount of added acetic acid on the hydrogel mechanical properties via the cantilever sensor response. The sensor resonance amplitude (A) decreased over mass ratios of M-Alg to PEI from 1:1 to 1:9 (Fig. S4), indicating that gelation occurred across a wide range of mass ratios. The shear storage modulus of the M-Alg/PEI hydrogels was also tunable by changing the amount of acetic acid added to catalyze the gelation process (Fig. S5). For example, resonance amplitude decreased as the volume of catalytic acetic acid was increased (5, 10, or 15 μL). This result is consistent with the fact that more amine groups will be protonated as more acetic acid is added, inducing stronger ionic interactions, and with the fact that the amount of catalyst for imine formation is increasing (but it is also a catalyst for imine hydrolysis). Using a fluid-structure interaction model (Mather et al., 2012), the relationship between the shear storage modulus (G') and hydrogel composition was obtained. Fig. 5 shows that the effect of mass ratio and acetic acid amount on the hydrogel mechanical properties, specifically G'. G' was sensitive to the mass ratio of M-Alg to PEI, reaching a maximum at maximum proportion

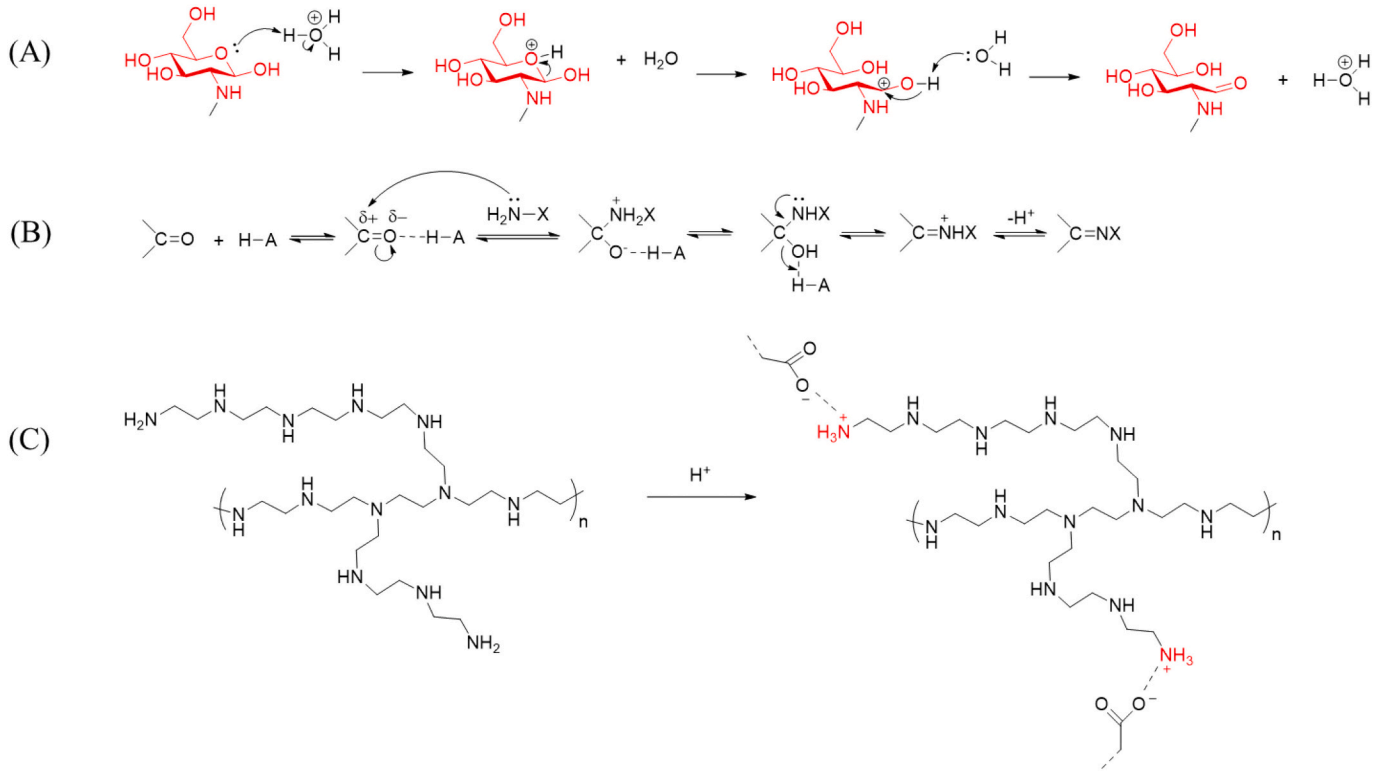

Fig. 1. (A) Mechanism of hydrogen-ion catalyzed ring-opening of monosaccharide; (B) mechanism of acetic acid catalyzed Schiff base formation (H-A refers to acetic acid CH_3COOH); (C) mechanism of ionic interaction between protonated amine $–NH_3^+$ and $–COO^-$; (D, E) overall gelation mechanism.

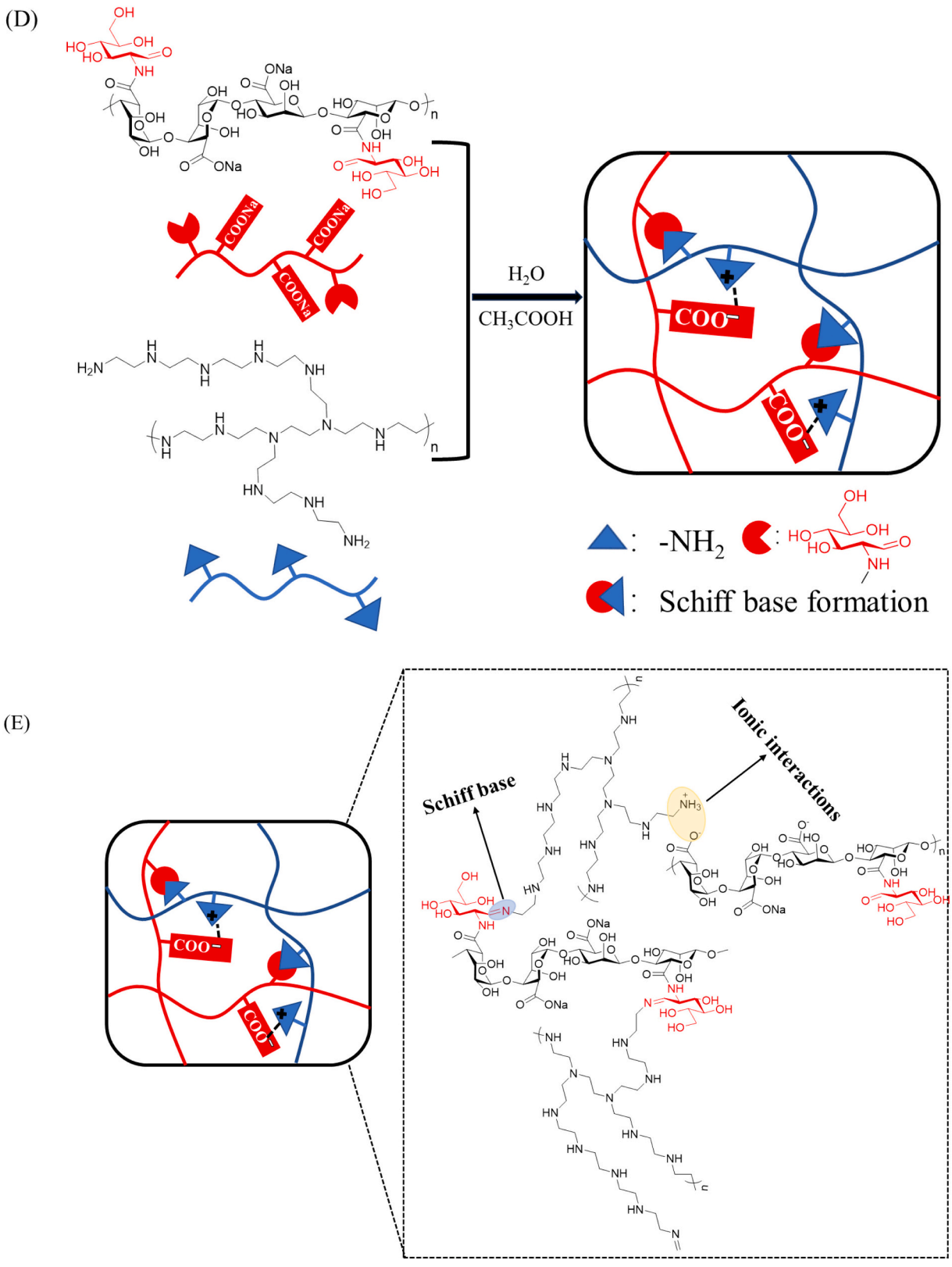

Fig. 1. (*continued*).

of PEI. Increasing the amount of acetic acid used for gelation also resulted in hydrogels of relatively higher G′, which is consistent with the results discussed in Section 3.1.

3.3. Self-healing and injectability

Due to their inferior mechanical properties compared to metals or ceramics, it is crucial that hydrogels possess self-healing properties so that they may repair any damage, thereby permitting longer lifetime and

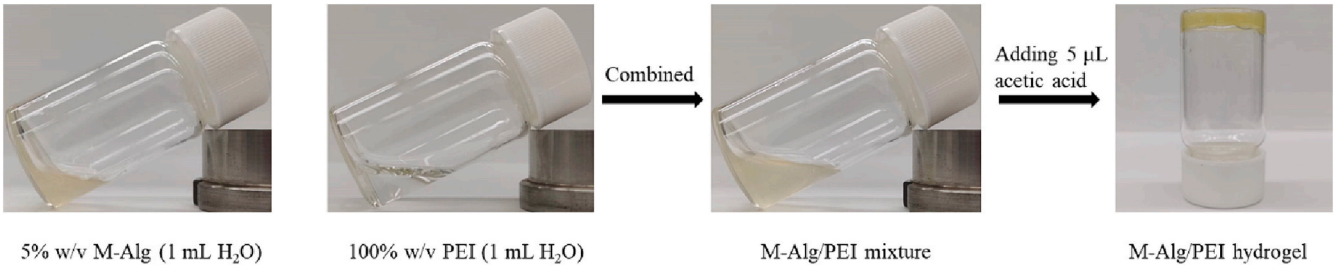

Fig. 2. Hydrogel formation between M-Alg and PEI solutions.

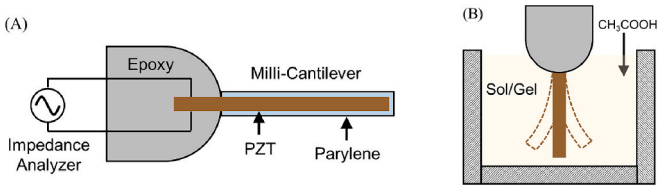

Fig. 3. (A) Schematic of a piezoelectric milli-cantilever rheometer; (B) low-volume measurement format for real-time monitoring of M-Alg/PEI gelation via viscoelastic property response.

better performance (Gyarmati et al., 2017). A rheometer in parallel plate geometry was used to examine the self-healing properties of M-Alg/PEI hydrogels under the small amplitude oscillatory shear (SAOS) mode. A frequency sweep experiment confirmed hydrogel formation ($G' > G''$) (Fig. 6a). The hydrogel linear viscoelastic region was determined by a strain sweep experiment (Fig. 6b). Self-healing performance was probed by an alternating step strain experiment (Fig. 6c). Alternating strains of 1 % and 100 % were applied to the hydrogel at 5-min intervals. The hydrogel transitioned from viscoelastic solid to viscoelastic liquid as strain increased from 1 % to 100 %, then recovered to its initial modulus. This behavior repeated, even after 5 cycles. At the same time, gradually increasing stiffness was observed (Fig. 6c), most likely attributed to water loss over the timescale of the experiment since a solvent trap was not available to control moisture loss. Self-healing behavior of M-Alg/PEI hydrogel was also demonstrated by cutting the hydrogel in the middle and placing the two pieces together without any pressure (Fig. 7). Due to the reversible and dynamic nature of Schiff-base bonds, the two pieces of M-Alg/PEI hydrogel self-healed into one piece within 12 h. Another demonstration of self-healing was carried out by preparing two gels and then placing them side by side. The two gels had merged such that they could be lifted as a single piece by spatula within 12 h (Fig. S6).

Injectability is of vital importance for hydrogel biomedical applications like drug delivery or tissue engineering, allowing for minimally invasive implantation (Pertici et al., 2019). Injectability was illustrated in simple, visual fashion by injecting M-Alg/PEI solutions to draw different pictures, shown in Fig. 8. The pictures were quickly resistant to flow after spraying a tiny amount of acetic acid on the surface of the applied hydrogel.

Low cytotoxicity is crucial for potential biomedical application of hydrogels. Cell viability was tested using L929 cells, which were incubated with different concentrations of M-Alg and PEI DMEM solutions (Fig. S8). M-Alg exhibited almost no harm to the cells up to 10 mg/mL. This was consistent with our hypothesis that attaching glucosamines to alginate chains would not alter their benign nature. PEI exhibited severe cytotoxicity to cells even at concentrations as low as 20 µg/mL, which is

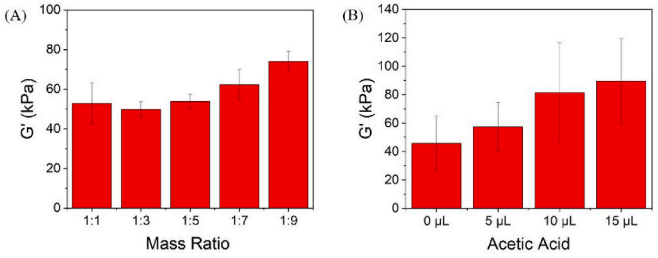

Fig. 5. Effect of mass ratio (M-Alg:PEI) (A) and acetic acid amount (B) on hydrogel G′ obtained from sensor response and a fluid-structure interaction model.

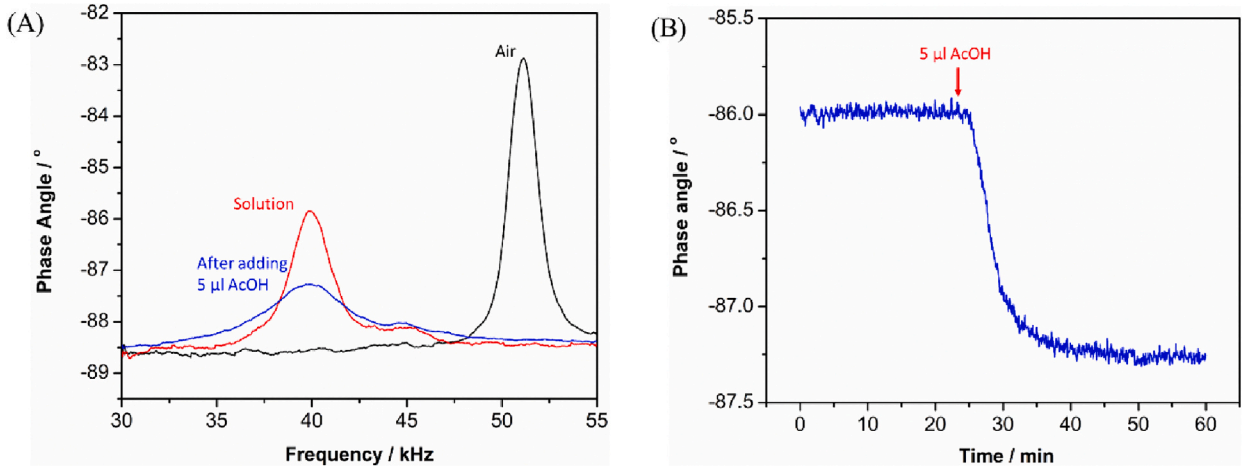

Fig. 4. (A) Cantilever sensor frequency response in terms of phase angle as measured by electrical impedance analysis in air (black curve), solution (red curve), and M-Alg/PEI hydrogel (blue curve); (B) real-time monitoring of M-Alg/PEI hydrogel gelation via continuous tracking of PEM phase angle at resonance (Φ). (For interpretation of the references to color in this figure legend, the reader is referred to the web version of this article.)

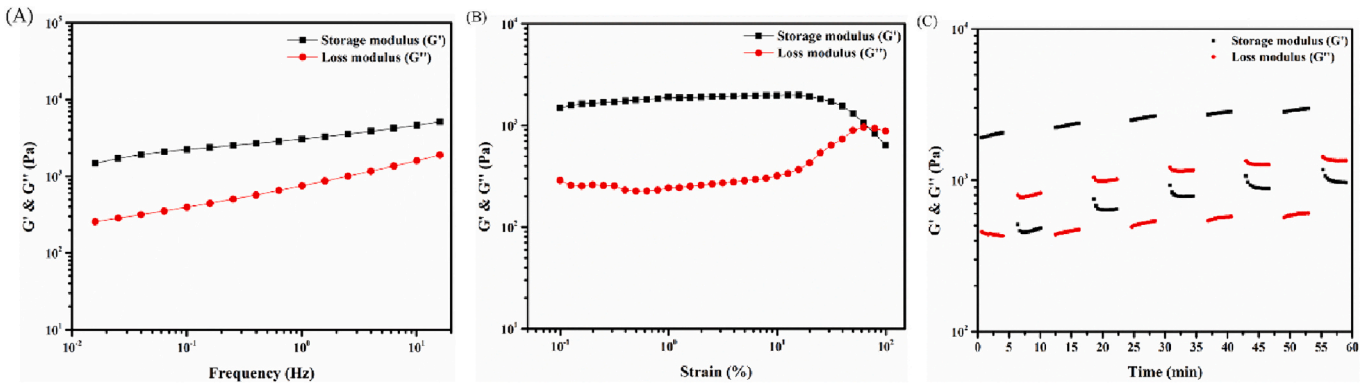

Fig. 6. (A) frequency sweep (1 % strain); (B) strain sweep (0.1 Hz); (C) step-strain sweep (0.1 Hz; alternating between 1 % strain and 100 % strain at 5 min intervals).

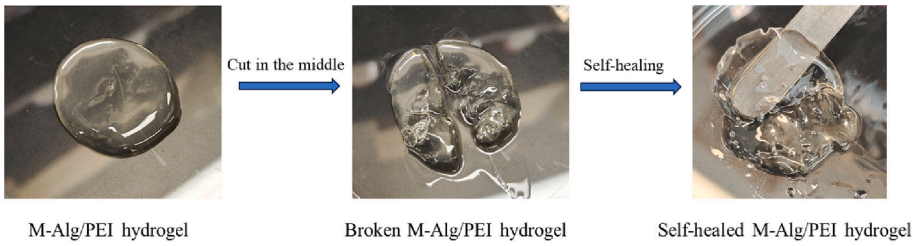

Fig. 7. Self-healing behavior of M-Alg/PEI hydrogel.

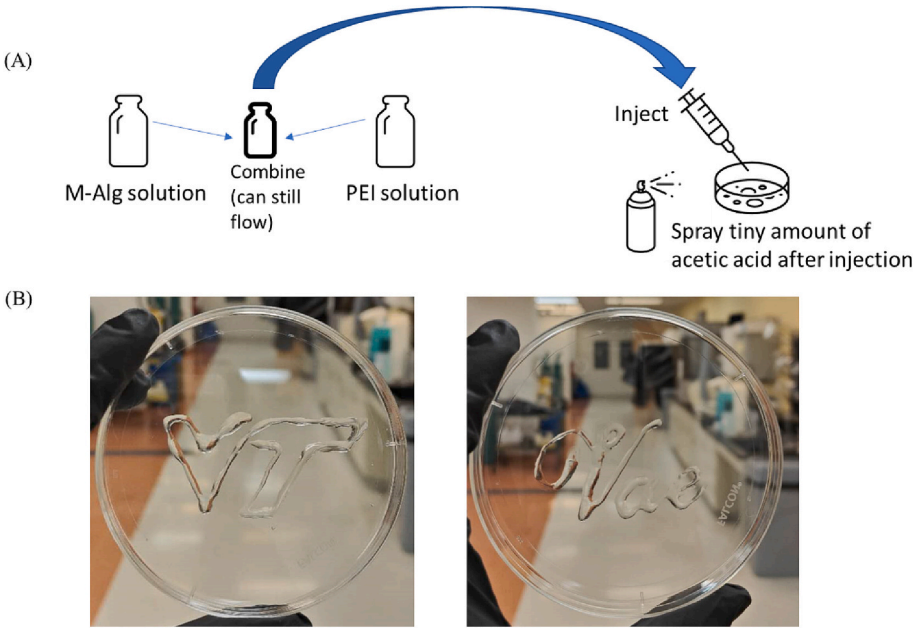

Fig. 8. (A) Schematic illustration of injectability of hydrogels. (B) Virginia Tech logo (left) and the name of the first author's favorite singer from China (right) drawn by injection of polymer mixture and cured by spraying a small amount of acetic acid solution.

consistent with previous studies (Brunot et al., 2007; Khansarizadeh et al., 2015; Moghimi et al., 2005). By combing M-Alg with PEI to form hydrogels, cytotoxicity was suppressed (Fig. 9). After seeding the L929 cells on the top of M-Alg/PEI hydrogels for a variety of time periods (1 h, 5 h and 24 h), only a few dead cells (red fluorescence, stained by ethidium homodimer) were observed, supporting the possibility that the toxicity of these M-Alg/PEI hydrogels may be sufficiently low for biomedical applications, and indicating that PEI toxicity was moderated by inclusion in these hydrogels (even though the connecting bonds are dynamic). For future studies, more benign amine polymers such as polylysine or amine-terminated polyethylene oxide (amine-PEO) can be considered to further improve the compatibility of hydrogels based on multi-reducing end polysaccharides (MREPs) with living cells in medically pertinent situations.

4. Conclusions

In this work, a self-healing, injectable, fast-gelling hydrogel based on multi-reducing end alginate (M-Alg) has been developed using acetic acid to accelerate the gelation process. Multi-reducing end alginate (M-

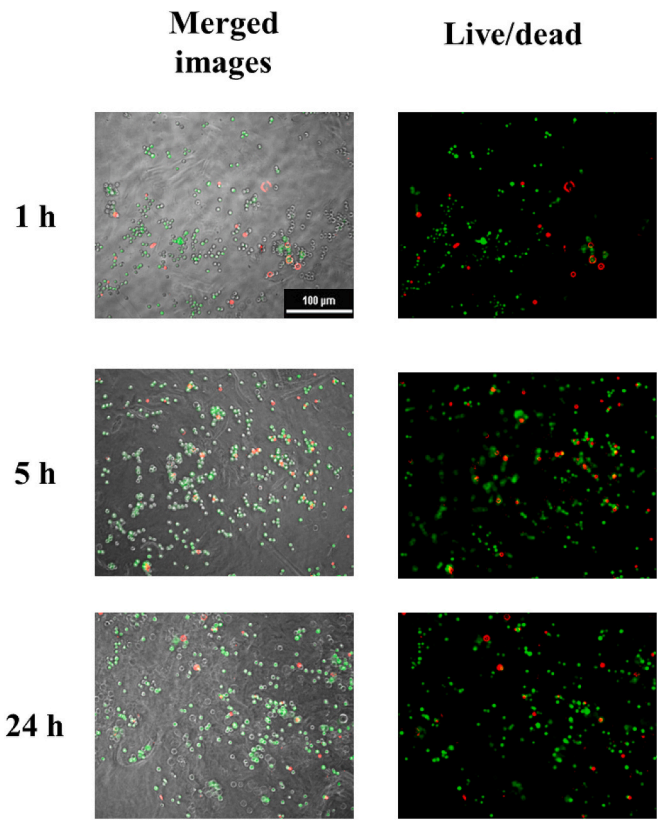

Fig. 9. Representative merged bright field and live/dead images of L929 cells seeding on top of the M-Alg/PEI hydrogels (live = green; red = dead). (For interpretation of the references to color in this figure legend, the reader is referred to the web version of this article.)

Alg) can form hydrogels with polyethyleneimine (PEI) at room temperature, while alginate cannot. Trace amounts of acetic acid can be used to accelerate gelation time from hours to seconds. The fast gelation behavior of M-Alg/PEI hydrogel was confirmed by real-time monitoring of viscoelastic properties employing a milli-cantilever rheometer. Self-healing and injectable properties were authenticated using parallel-plate rheology, as well as by visual observation of hydrogels applied by syringe. Overall, this work provides powerful insights that support the application potential of multi-reducing end polysaccharides (MREPs). Hydrogels based on MREPs are promising for many biomedical applications. For example, many cancer tissues have an acidic environment. Hydrogels based on MREPs can load one or more anticancer drugs and be injected to the site of the cancer cells. The acidic environment will induce fast gelation of MREPs hydrogels for controlled drug release, creating the potential to localize treatment exactly where it is needed, and minimize off-target side effects. We continue to explore such applications for these hydrogels.

CRediT authorship contribution statement

Zhenghao Zhai: Writing – review & editing, Writing – original draft, Visualization, Validation, Methodology, Investigation, Formal analysis, Conceptualization. **Yang Zhou:** Conceptualization, Methodology, Investigation, Validation, Formal analysis, Visualization, Writing - review & editing. **Ishani Sarkar:** Writing – review & editing, Validation, Investigation. **Yang Liu:** Writing – review & editing, Visualization, Validation, Methodology, Investigation, Formal analysis, Conceptualization. **Yimin Yao:** Writing – review & editing, Validation, Investigation. **Junru Zhang:** Investigation. **Michael J. Bortner:** Writing – review & editing, Validation, Investigation, Formal analysis. **John B. Matson:** Writing – review & editing, Visualization, Resources, Investigation, Formal analysis. **Blake N. Johnson:** Writing – review & editing, Validation, Investigation, Formal analysis. **Kevin J. Edgar:** Writing – review & editing, Writing – original draft, Supervision, Resources, Methodology, Investigation.

Declaration of competing interest

The authors report no competing interests.

Data availability

Data will be made available on request.

Acknowledgements

We thank the Virginia Tech Institute for Critical Technology and Applied Science, and the Macromolecules Innovation Institute for partial support of this work. We are grateful for the U. S. Department of Agriculture (NIFA) for support of this work through grant 2020-67021-31379 (ZZ). We thank Dr. Irving Coy Allen for providing the L929 cells and for support from grant NSF (IS; CHE-2003662). We thank Dr. Murthy Shanaiah for guidance about NMR experiments. This work was partially supported by GlycoMIP, a National Science Foundation Materials Innovation Platform funded through Cooperative Agreement DMR-1933525.

Appendix A. Supplementary data

Supplementary data to this article can be found online at https://doi.org/10.1016/j.carbpol.2024.122172.

References

Alonso, J. M., Del Olmo, J. A., Gonzalez, R. P., & Saez-martinez, V. (2021). Injectable hydrogels: From laboratory to industrialization. In , *Vol. 13*. *Polymers* (pp. 1–24). MDPI AG. https://doi.org/10.3390/polym13040650. Issue 4.

Brunot, C., Ponsonnet, L., Lagneau, C., Farge, P., Picart, C., & Grosgogeat, B. (2007). Cytotoxicity of polyethyleneimine (PEI), precursor base layer of polyelectrolyte multilayer films. *Biomaterials, 28*(4), 632–640. https://doi.org/10.1016/j.biomaterials.2006.09.026

Cesewski, E., Singh, M., Liu, Y., Zhang, J., Haring, A. P., & Johnson, B. N. (2020). Real-time monitoring of hydrogel rheological property changes and gelation processes using high-order modes of cantilever sensors. *Journal of Applied Physics, 128*(17). https://doi.org/10.1063/5.0020547

Chen, J., Nichols, B. L. B., Norris, A. M., Frazier, C. E., & Edgar, K. J. (2020). All-polysaccharide, self-healing injectable hydrogels based on chitosan and oxidized hydroxypropyl polysaccharides. *Biomacromolecules, 21*(10), 4261–4272. https://doi.org/10.1021/acs.biomac.0c01046

Chen, J., Zhai, Z., & Edgar, K. J. (2022). Recent advances in polysaccharide-based in situ forming hydrogels. *Current Opinion in Chemical Biology, 70*, Article 102200. https://doi.org/10.1016/j.cbpa.2022.102200

Cordes, E. H., & Jencks, W. P. (1962). On the mechanism of Schiff base formation and hydrolysis. *Journal of the American Chemical Society, 84*(5), 832–837. https://doi.org/10.1021/ja00864a031

Dimatteo, R., Darling, N. J., & Segura, T. (2018). In situ forming injectable hydrogels for drug delivery and wound repair. In , *Vol. 127*. *Advanced drug delivery reviews* (pp. 167–184). Elsevier B.V. https://doi.org/10.1016/j.addr.2018.03.007.

Drury, J. L., & Mooney, D. J. (2003). Hydrogels for tissue engineering: Scaffold design variables and applications. *Biomaterials, 24*(24), 4337–4351. https://doi.org/10.1016/S0142-9612(03)00340-5

Guvendiren, M., Lu, H. D., & Burdick, J. A. (2012). Shear-thinning hydrogels for biomedical applications. *Soft Matter, 8*(2), 260–272. https://doi.org/10.1039/C1SM06513K

Gyarmati, B., Szilágyi, B.Á., & Szilágyi, A. (2017). Reversible interactions in self-healing and shape memory hydrogels. *European Polymer Journal, 93*, 642–669. https://doi.org/10.1016/j.eurpolymj.2017.05.020

Haring, A. P., Singh, M., Koh, M., Cesewski, E., Dillard, D. A., Kong, Z. J., & Johnson, B. N. (2020). Real-time characterization of hydrogel viscoelastic properties and sol-gel phase transitions using cantilever sensors. *Journal of Rheology, 64*(4), 837–850. https://doi.org/10.1122/8.0000009

Hoare, T. R., & Kohane, D. S. (2008). Hydrogels in drug delivery: Progress and challenges. *Polymer, 49*(8), 1993–2007. https://doi.org/10.1016/j.polymer.2008.01.027

Hozumi, T., Kageyama, T., Ohta, S., Fukuda, J., & Ito, T. (2018). Injectable hydrogel with slow degradability composed of gelatin and hyaluronic acid cross-linked by Schiff's

base formation. *Biomacromolecules, 19*(2), 288–297. https://doi.org/10.1021/acs.biomac.7b01133
Khansarizadeh, M., Mokhtarzadeh, A., Rashedinia, M., Taghdisi, S. M., Lari, P., Abnous, K. H., & Ramezani, M. (2015). Identification of possible cytotoxicity mechanism of polyethylenimine by proteomics analysis. *Human & Experimental Toxicology, 35*(4), 377–387. https://doi.org/10.1177/0960327115591371
Kong, H. J., & Mooney, D. J. (2003). The effects of poly(ethyleneimine) (PEI) molecular weight on reinforcement of alginate hydrogels. In *, Vol. 12. Cell transplantation*. www.cognizantcommunication.com.
Kristiansen, K. A., Potthast, A., & Christensen, B. E. (2010). Periodate oxidation of polysaccharides for modification of chemical and physical properties. *Carbohydrate Research, 345*(10), 1264–1271. https://doi.org/10.1016/j.carres.2010.02.011
Lee, K. Y., & Mooney, D. J. (2001). Hydrogels for tissue engineering. *Chemical Reviews, 101*(7), 1869–1880. https://doi.org/10.1021/cr000108x
Li, J., & Mooney, D. J. (2016). Designing hydrogels for controlled drug delivery. *Nature Reviews Materials, 1*(12), 16071. https://doi.org/10.1038/natrevmats.2016.71
Liu, Y., Bethel, K., Singh, M., Zhang, J., Ashkar, R., Davis, E. M., & Johnson, B. N. (2022). Comparison of bulk- vs layer-by-layer-cured stimuli-responsive PNIPAM–alginate hydrogel dynamic viscoelastic property response via embedded sensors. *ACS Applied Polymer Materials, 4*(8), 5596–5607. https://doi.org/10.1021/acsapm.2c00634
Malik, U. S., Niazi, M. B. K., Jahan, Z., Zafar, M. I., Vo, D. V. N., & Sher, F. (2022). Nano-structured dynamic Schiff base cues as robust self-healing polymers for biomedical and tissue engineering applications: A review. In *, Vol. 20. Environmental chemistry letters* (pp. 495–517). Springer Science and Business Media Deutschland GmbH. https://doi.org/10.1007/s10311-021-01337-1. Issue 1.
Mather, M. L., Rides, M., Allen, C. R. G., & Tomlins, P. E. (2012). Liquid viscoelasticity probed by a mesoscale piezoelectric bimorph cantilever. *Journal of Rheology, 56*(1), 99–112. https://doi.org/10.1122/1.3670732
Mo, C., Xiang, L., & Chen, Y. (2021). Advances in injectable and self-healing polysaccharide hydrogel based on the Schiff Base reaction. In *, Vol. 42. Macromolecular rapid communications*. John Wiley and Sons Inc.. https://doi.org/10.1002/marc.202100025. Issue 10.
Moghimi, S. M., Symonds, P., Murray, J. C., Hunter, A. C., Debska, G., & Szewczyk, A. (2005). A two-stage poly(ethylenimine)-mediated cytotoxicity: Implications for gene transfer/therapy. *Molecular Therapy, 11*(6), 990–995. https://doi.org/10.1016/j.ymthe.2005.02.010
Pan, Z., Ye, H., & Wu, D. (2021). Recent advances on polymeric hydrogels as wound dressings. In *, Vol. 5. APL bioengineering*. American Institute of Physics Inc.. https://doi.org/10.1063/5.0038364. Issue 1.
Patenaude, M., Campbell, S., Kinio, D., & Hoare, T. (2014). Tuning gelation time and morphology of injectable hydrogels using ketone–hydrazide cross-linking. *Biomacromolecules, 15*(3), 781–790. https://doi.org/10.1021/bm401615d
Pertici, V., Pin-Barre, C., Rivera, C., Pellegrino, C., Laurin, J., Gigmes, D., & Trimaille, T. (2019). Degradable and injectable hydrogel for drug delivery in soft tissues. *Biomacromolecules, 20*(1), 149–163. https://doi.org/10.1021/acs.biomac.8b01242
Qian, X. (2013). Free energy surface for Brønsted acid-catalyzed glucose ring-opening in aqueous solution. *Journal of Physical Chemistry B, 117*(39), 11460–11465. https://doi.org/10.1021/jp402739q
Rajabi, M., McConnell, M., Cabral, J., & Ali, M. A. (2021). Chitosan hydrogels in 3D printing for biomedical applications. In *, Vol. 260. Carbohydrate polymers*. Elsevier Ltd.. https://doi.org/10.1016/j.carbpol.2021.117768
Santerre, G. M., Hansrote, C. J., Jr., & Crowell, T. I. (1958). The reaction of aromatic aldehydes with n-butylamine. Acid catalysis and substituent effects. *Journal of the American Chemical Society, 80*(5), 1254–1257. https://doi.org/10.1021/ja01538a056
Sharma, H., Lakshmanan, R. S., Johnson, B. N., & Mutharasan, R. (2011). Piezoelectric cantilever sensors with asymmetric anchor exhibit picogram sensitivity in liquids. *Sensors and Actuators B: Chemical, 153*(1), 64–70. https://doi.org/10.1016/j.snb.2010.10.006
Shen, W., Zhang, K., Kornfield, J. A., & Tirrell, D. A. (2006). Tuning the erosion rate of artificial protein hydrogels through control of network topology. *Nature Materials, 5*(2), 153–158. https://doi.org/10.1038/nmat1573
Singh, M., Zhang, J., Bethel, K., Liu, Y., Davis, E. M., Zeng, H., … Johnson, B. N. (2021). Closed-loop controlled photopolymerization of hydrogels. *ACS Applied Materials and Interfaces, 13*(34), 40365–40378. https://doi.org/10.1021/acsami.1c11779
Sun, Y., Nan, D., Jin, H., & Qu, X. (2020). Recent advances of injectable hydrogels for drug delivery and tissue engineering applications. *Polymer Testing, 81*, Article 106283. https://doi.org/10.1016/j.polymertesting.2019.106283
Tavakoli, S., & Klar, A. S. (2020). Advanced hydrogels as wound dressings. In *, Vol. 10. Biomolecules* (pp. 1–20). MDPI AG. https://doi.org/10.3390/biom10081169. Issue 8.
Tian, B., Hua, S., Tian, Y., & Liu, J. (2020). Chemical and physical chitosan hydrogels as prospective carriers for drug delivery: A review. *Journal of Materials Chemistry B, 8*(44), 10050–10064. https://doi.org/10.1039/d0tb01869d
Yang, C., Gao, L., Liu, X., Yang, T., Yin, G., Chen, J., Guo, H., Yu, B., & Cong, H. (2019). Injectable Schiff base polysaccharide hydrogels for intraocular drug loading and release. *Journal of Biomedical Materials Research — Part A, 107*(9), 1909–1916. https://doi.org/10.1002/jbm.a.36677
Yang, Y., Xu, L., Wang, J., Meng, Q., Zhong, S., Gao, Y., & Cui, X. (2022). Recent advances in polysaccharide-based self-healing hydrogels for biomedical applications. *Carbohydrate Polymers, 283*, Article 119161. https://doi.org/10.1016/j.carbpol.2022.119161
Yue, X., Al Kontar, R., Berahas, A. S., Liu, Y., Zai, Z., Edgar, K., & Johnson, B. N. (2023). Collaborative and distributed Bayesian optimization via consensus: Showcasing the power of collaboration for optimal design. http://arxiv.org/abs/2306.14348.
Zhai, Z., Zhou, Y., Korovich, A. G., Hall, B. A., Yoon, H. Y., Yao, Y., … Edgar, K. J. (2023). Synthesis and characterization of multi-reducing-end polysaccharides. *Biomacromolecules, 24*(6), 2596–2605. https://doi.org/10.1021/acs.biomac.3c00104
Zhang, J., Liu, Y., Chandra Sekhar, P. D., Singh, M., Tong, Y., Kucukdeger, E., … Johnson, B. N. (2023). Rapid, autonomous high-throughput characterization of hydrogel rheological properties via automated sensing and physics-guided machine learning. *Applied Materials Today, 30*. https://doi.org/10.1016/j.apmt.2022.101720
Zhou, Y., Zhai, Z., Yao, Y., Stant, J. C., Landrum, S. L., Bortner, M. J., … Edgar, K. J. (2023). Oxidized hydroxypropyl cellulose/carboxymethyl chitosan hydrogels permit pH-responsive, targeted drug release. *Carbohydrate Polymers, 300*, Article 120213. https://doi.org/10.1016/j.carbpol.2022.120213